Chinese Chemical Letters 37 (2026) 111209

Contents lists available at ScienceDirect

Chinese Chemical Letters

journal homepage: www.elsevier.com/locate/cclet

Simultaneous removal of tetracycline and antibiotic resistant bacteria/genes in UV-LED/H_2O_2 system: Competitive interactions and wavelength dependence

Jie Wang[a], Jijie Zhang[a], Defang Ma[a], Zhenxiang Sun[a], Yan Wang[a], Qinyan Yue[a], Yanwei Li[b], Yue Gao[a,*], Baoyu Gao[a,*], Xing Xu[a]

[a] Key Laboratory of Water Pollution Control and Recycling (Shandong), School of Environmental Science and Engineering, Shandong University, Qingdao 266237, China
[b] Environment Research Institute, Shandong University, Qingdao 266237, China

ARTICLE INFO

Article history:
Received 11 December 2024
Revised 8 February 2025
Accepted 14 April 2025
Available online 15 April 2025

Keywords:
UV-LED/H_2O_2
ARB/ARGs
Wavelength dependence
Competition
Simultaneous removal

ABSTRACT

The coexistence of emerging containments, such as antibiotic resistant bacteria (ARB), antibiotic-resistant genes (ARGs) and antibiotics, potentially influence elimination efficiencies in UV light-emitting diode (UV-LED) alone and UV-LED/H_2O_2 system as their complex interactions. Tetracycline (TC) degradation efficiency (k_F) correlated closely with its UV molar absorbance ($R^2 = 0.831$) in UV-LED alone system and with $^{\bullet}OH$ yield ($R^2 = 0.999$) in UV-LED/H_2O_2 system across studied wavelengths (265, 280 and 310 nm). The k_F values for intracellular DNA (i-ARGs) also exhibited a high correlation with UV-LED wavelengths in both systems ($R^2 = 0.997$–0.999). The coexistence of TC and ARB/ARGs resulted in a mutual inhibition of their degradation efficiencies due to competition for photons and $^{\bullet}OH$, along with the consequent reduction in intracellular ROS within ARB, with their degradation efficiencies exhibiting marked dependence on wavelength in both systems. Notably, the UV-LED/H_2O_2 system at 265 nm effectively achieved the simultaneous removal of TC, ARB and ARGs with minimal energy consumption, and successfully fragmented ARGs. The degradation pathway of TC was analyzed, and the biotoxicity of its degradation intermediates demonstrated the environmental friendliness and safety of UV-LED/H_2O_2 technology. This study elucidated the competitive interactions between antibiotics and ARB/ARGs within UV-LED/H_2O_2 system, providing a promising approach for their simultaneous removal while ensuring energy efficiency.

© 2025 Published by Elsevier B.V. on behalf of Chinese Chemical Society and Institute of Materia Medica, Chinese Academy of Medical Sciences.

The widespread use of antibiotics in medicine, livestock farming, and aquaculture has resulted in global pollution and adverse effects, posing serious risks to public health and the environment [1,2]. The emergence of antibiotic-resistant bacteria (ARB) and antibiotic-resistant genes (ARGs) as new pollutants in various environmental matrices has further heightened these concerns [3]. The ARB can perpetuate ARGs through vertical gene transfer, passing these ARGs to subsequent generations. In addition, ARGs can propagate *via* horizontal gene transfer, enabling rapid adaptation to environmental changes, contributing to the proliferation of ARB and ARGs, ultimately facilitating the emergence of multi-drug resistant superbugs [4–6]. Antibiotic residues in environment can enhance the resistance of ARB, and the coexistence of antibiotics and ARGs greatly accelerate the proliferation of ARGs within ARB [7,8]. Therefore, the simultaneous removal of antibiotics, ARB and ARGs is critical.

Advanced oxidation processes (AOPs) have proven effective in eliminating antibiotics and ARB/ARGs [9,10]. Among these, UV based AOPs are widely employed in sewage treatment for sterilization and antibiotic removal, with UV/chlorine technology being the most common [11]. However, the UV/chlorine process commonly produces a series of disinfection by-products, some of which are carcinogenic and pose health risks [12–14]. The UV/H_2O_2 system provides a promising solution for this issue, owing to its high efficiency and environmentally friendly characteristics [12]. Recently, UV light-emitting diode (UV-LED) has garnered significant attention as an emerging UV light source, providing advantages such as multiple emission wavelengths, longer lifespan, low energy consumption, and flexibility, while being mercury-free [15,16]. These features position UV-LED as a promising replacement for traditional low-pressure UV mercury lamps (LPUV), overcoming their limitations [15,17].

* Corresponding authors.
E-mail addresses: ygao@sdu.edu.cn (Y. Gao), baoyugao_sdu@aliyun.com (B. Gao).

https://doi.org/10.1016/j.cclet.2025.111209
1001-8417/© 2025 Published by Elsevier B.V. on behalf of Chinese Chemical Society and Institute of Materia Medica, Chinese Academy of Medical Sciences.

The UV-LED irradiation disrupts the structure of microbial deoxyribonucleic acid (DNA), leading to the immediate inactivation of ARB or inhibiting their reproduction, thereby ensuring effective disinfection [18]. In UV-LED/H_2O_2 system, hydroxyl radicals (•OH), as the primary reactive oxygen species (ROS), attack the DNA base of ARGs, causing double-strand breaks that contribute to their removal [19]. In addition, the antibiotics are degraded through direct photolysis by UV light in UV-LED alone system and electrophilic attack by •OH in UV-LED/H_2O_2 system [20]. However, competition for UV photons and •OH between antibiotic and ARB/ARGs complicates their simultaneous removal, posing a critical challenge. Therefore, the primary objective was to achieve the simultaneous removal of antibiotics and ARB/ARGs, while elucidating the competitive mechanisms influencing their degradation.

Tetracyclines are extensively utilized in medical treatment, livestock farming, and agricultural production due to their broad-spectrum antimicrobial activity and cost-efficiency [21]. The persistence of tetracyclines in wastewater has raised concerns, as it contributes to the emergence of ARB/ARGs, posing substantial threats to both human health and environmental ecosystems [22,23]. In this study, tetracycline (TC) as the most common tetracyclines was selected to evaluate the interrelationship between TC, and TC-associated ARB/ARGs in terms of degradation efficiency within UV-LED alone and UV-LED/H_2O_2 system. The wavelength dependence on TC, ARB and ARGs elimination efficiencies were evaluated at 265, 280 and 310 nm for both systems. The effects of wavelength and coexistence of ARB/ARGs on energy consumption in UV-LED/H_2O_2 system were evaluated. The UV-LED/H_2O_2 system at 265 nm achieved simultaneous removal of TC and ARB/ARGs, demonstrating significant energy efficiency, with the fragmentation of ARGs also observed. Finally, the degradation pathway of TC and biotoxicity of its degradation intermediates were explored in UV-LED/H_2O_2 system, confirming its environmental friendliness. This study provided a comprehensive understanding of the interactions and mechanisms influencing the removal of antibiotics and ARB/ARGs, providing novel insights into their synchronous elimination.

The hazards associated with ARB and ARGs originating from antibiotic wastewater emphasized the critical need for their simultaneous elimination to minimize their mutual influence. The degradation efficiency of TC was first investigated in UV-LED alone and UV-LED/H_2O_2 systems at wavelengths of 265, 280 and 310 nm, while also evaluating the impact of ARB on TC removal. The wavelength of the UV-LED played a crucial role in determining the electronic excitation of antibiotics and H_2O_2 molecules, directly impacting the efficiency of TC degradation [24]. As shown in Fig. S1b (Supporting information), the UV-LED light with the wavelengths less than 310 nm was easily absorbed by H_2O_2, whereas wavelengths longer than 310 nm exhibited minimal adsorption. While UV-LEDs with shorter wavelengths, such as lower than 260 nm, were known for their potential in disinfection and wastewater treatment, limitations in current production technology result in low power output and weak light intensity. These limitations contributed to poor time-based degradation efficiency (k_{obs}) and introduced significant errors in UV photon fluence-based rate constant (k_F) calculations, as observed in our previous studies [25,26]. To ensure accurate and reliable results, UV-LEDs with more commonly used wavelengths (265, 280, and 310 nm) were selected for wavelength dependence investigation on TC removal. For UV based AOPs, the k_F represented the degradation efficiency of organic pollutants under unit exposure photon fluence. Unlike the k_{obs}, k_F was independent of UV-LED irradiance, making it a more suitable and scientifically parameter for evaluating both the activation efficiency of H_2O_2 across different UV-LED wavelength and the overall wastewater treatment performance [26]. According to the UV-LED irradiance at various wavelengths (I_s, Table S1 in Supporting information), k_F could be calculated as k_{obs}/I_s, and details were provided in Support information.

The TC exhibited considerable resistance to degradation in H_2O_2 alone system in 0.9% NaCl solution, regardless of the ARB coexist (Fig. S2 in Supporting information). The 0.9% NaCl solution provided a stable, neutral, and physiologically compatible environment that supported ARB cellular activity and function. The k_{obs} and k_F both followed the order of 280, 265 and 310 nm in UV-LED alone system, while the UV-LED/H_2O_2 system exhibited the order of 265, 280 and 310 nm (Figs. 1a-e and Fig. S3 in Supporting information). The UV-LED/H_2O_2 system significantly improved the TC degradation efficiency, achieving an increase of 4.36–16.85 times compared to the UV-LED alone system (Figs. 1d and e). The coexistence of ARB led to a reduction of the k_F values in by 33.6%–44.5% in UV-LED alone system and by 14.3%–53.2% in UV-LED/H_2O_2 system (Figs. 1d and e), with corresponding decreases in removal rates of 6.5%–14.6% at 120 min (Fig. 1f). The ethanol (EtOH) was employed as the quencher for •OH, effectively inhibiting TC degradation in UV-LED/H_2O_2 system across three studied wavelengths, thereby confirming that •OH was the primary ROS (Fig. S4 in Supporting information). The electron paramagnetic resonance (EPR) spectra confirmed the generation of •OH in UV-LED/H_2O_2 system (Fig. S5a in Supporting information), with intensity decreasing in the order of 265, 280 and 310 nm, due to the increased UV molar absorbance (ε_λ) of H_2O_2 at shorter UV-LED wavelengths (Fig. S1b) [25]. In order to facilitate a direct comparison of •OH generation across three wavelengths, the •OH signal intensity was standardized to fluence-based •OH intensity based on the UV-LED irradiance (W/m^2, Table S1). The fluence-based •OH intensity also exhibited the same trend, with the highest intensity observed at 265 nm (Fig. S5b in Supporting information). The fluence-based •OH intensity should a strong correlation with the k_F for TC degradation ($R^2 = 0.996$) (Fig. 1g). In addition, in UV-LED alone system, the ε_λ of pollutants at various wavelengths directly influenced their photochemical degradation efficiency by determining the UV-LED light absorption and molecular excitation [3,27]. Strong linear correlations were observed between k_F at three studied wavelengths and the corresponding ε_λ for TC ($R^2 = 0.831$) in UV-LED alone system (Fig. 1h and Fig. S6a in Supporting information). These findings suggested that UV photolysis and •OH direct oxidation were the predominant mechanisms driving TC degradation in UV-LED alone and UV-LED/H_2O_2 systems, respectively (Figs. 1g and h), which consistent with our previous studies [25,28]. The order difference in TC degradation efficiency (Figs. 1d and e) in UV-LED alone and UV-LED/H_2O_2 systems at three studied wavelengths was attributed to the distinct degradation mechanisms inherent to each system. The lower k_F values and similar correlations in UV-LED alone ($R^2 = 0.670$) and UV-LED/H_2O_2 ($R^2 = 0.983$) systems with ARB coexistence indicated the competition for photons and •OH, respectively. Nevertheless, the UV-LED/H_2O_2 system at 265 nm demonstrated promising potential for TC removal, achieving 87.8% even in the presence of ARB.

Additionally, the energy consumption associated with the UV-LED/H_2O_2 system for TC degradation was analyzed, with a focus on the impact of UV-LED wavelengths and the presence of ARB (Fig. 1i). The electrical energy per order (EEO, kWh m^{-3} order^{-1}) was defined as the electric energy required to achieve a 90% reduction in pollutant concentration [25]. The ε_λ of pollutants and the photolysis efficiency of various oxidants exhibited significant variability across different UV wavelengths, thereby the EEO analysis in UV based AOPs was necessary. The EEO for TC degradation in UV-LED alone system was lowest at 280 nm, followed by 265 nm and 310 nm, aligning with the TC degradation efficiency (Fig. S6b in Supporting information). The photolysis efficiency of H_2O_2, •OH yield and TC degradation efficiency all decreased with increasing wavelength in UV-LED/H_2O_2 system, resulting in a corresponding

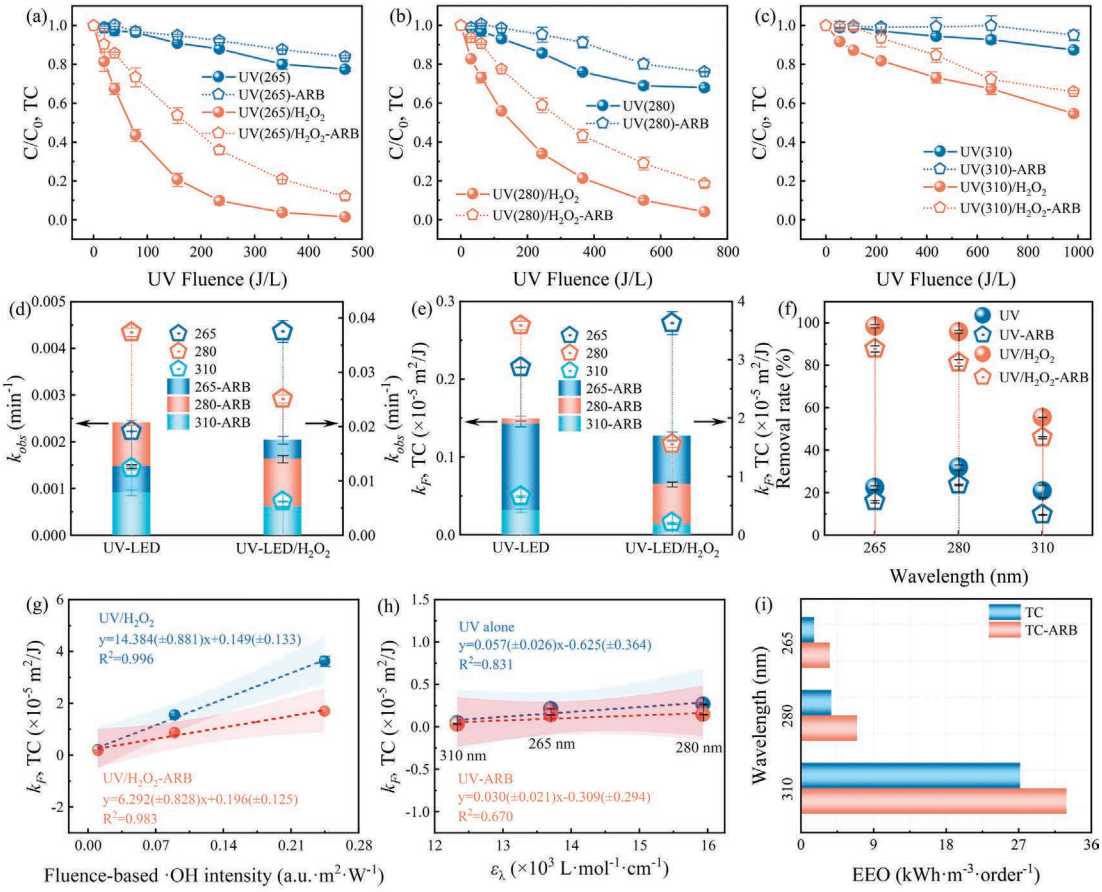


Fig. 1. Degradation kinetics of TC in UV-LED alone and UV-LED/H_2O_2 systems with or without ARB coexistence at (a) 265 nm, (b) 280 nm and (c) 310 nm. (d) Time-based first-order rate constant (k_{obs}) and (e) fluence-based first-order rate constant (k_F) for TC in UV-LED alone and UV-LED/H_2O_2 systems. (f) Removal rate of TC in UV-LED alone and UV-LED/H_2O_2 systems at 120 min under studied three wavelengths. Correlations between the k_F with (g) fluence-based ·OH intensity in UV-LED/H_2O_2 system and (h) ε_λ of TC in UV-LED alone system. (i) The EEO comparison of TC removal in UV-LED/H_2O_2 system under studied three wavelengths with or without ARB. Experiment conditions: TC 30 μmol/L, H_2O_2 10 mmol/L, ARB 3.5×10^6 CFU/mL, 0.9% NaCl solution.

trend in EEO. The presence of ARB significantly increased the energy demand across all studied wavelengths, due to the competition between ARB and TC for UV irradiance and ·OH, which were essential for TC removal. Thus, the UV-LED operating at 265 nm was particularly effective for H_2O_2 activation and wastewater treatment.

The impact of UV-LED wavelength and the TC coexistence on ARB inactivation efficiency was systemically investigated in UV-LED alone and UV-LED/H_2O_2 systems. The H_2O_2 alone system demonstrated minimal effectiveness in ARB inactivation, regardless of whether TC was coexistence (Fig. S7a in Supporting information). Conversely, both the UV-LED alone and UV-LED/H_2O_2 systems achieved complete ARB inactivation under low UV fluence (<30 J/L) at wavelengths of 265 nm and 280 nm (Figs. 2a and b). The presence of TC slightly reduced ARB inactivation efficiency in UV-LED system, with this inhibition further mitigated in UV-LED/H_2O_2 system due to enhanced oxidative capability (insert of Figs. 2a and b). The UV-LED irradiation at 265 nm directly damaged cellular DNA, resulting in rapid inactivation of ARB [29]. In contrast, ARB inactivation at 280 nm was attributed to protein denaturation caused by the disruption of specific molecular components, particularly the conjugated double bonds within the aromatic rings of amino acids such as tyrosine (Tyr), phenylalanine (Phe), and tryptophan (Trp) [30]. The inactivation of ARB in UV-LED alone system at 310 nm was unsatisfactory (Fig. 2c). Previous studies had shown that long-wavelength UV (310 nm) primarily affected cell components involved in metabolic cycle, such as lipids and certain proteins, as well as ROS scavengers like catalases and superoxide dismutase. These damage could deactivate ARB by inducing intracellular ROS formation [29]. Despite a greatly improvement upon combining UV-LED at 310 nm with H_2O_2, it still fell short of expectations. This limited improvement could be attributed to the generation of ·OH in the extracellular environment, which also facilitated the releasing of intracellular DNA (i-ARGs) [31]. The coexistence of TC significantly inhibited ARB inactivation in both systems at 310 nm, highlighting its unfavorable wavelength for ARB inactivation.

To assess the wavelength dependence of i-ARGs removal efficiency in UV-LED alone and UV-LED/H_2O_2 systems across three studied UV emission wavelengths, a log-linear decay fitting analysis was conducted. The removal efficiency of i-ARGs was negligible in H_2O_2 alone system (Fig. S7b in Supporting information), but it was remarkable in UV-LED alone system at 265 and 280 nm (Figs. 3a and b), especially at 265 nm, whereas negligible elimination efficiency was observed under irradiance at 310 nm (Fig. 3c). The k_F for i-ARGs exhibited excellent linear correlations with UV-LED wavelengths in UV-LED alone ($R^2 = 0.999$) and UV-LED/H_2O_2 ($R^2 = 0.997$) systems within 265–310 nm (Figs. 3d-f), suggesting a clear wavelength dependence in i-ARGs removal [31]. The wavelength dependence elimination of ARGs could be attributed to direct DNA damage under short-wavelength UV irradiation, coupled with decreased UV light absorption of genetic material with increasing UV-LED wavelength [29]. The i-ARGs destructive efficiency in UV-LED/H_2O_2 system showed only a slight improvement

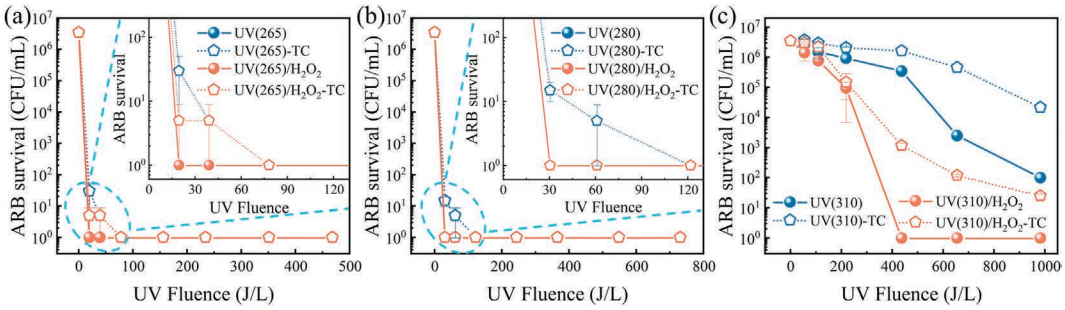


Fig. 2. The ARB survival with or without TC coexistence in UV-LED alone and UV-LED/H_2O_2 system at (a) 265 nm, (b) 280 nm and (c) 310 nm. The inset figures presented enlarged views of ARB survival under low UV fluence. Experiment conditions: TC 30 μmol/L, H_2O_2 10 mmol/L, ARB 3.5×10^6 CFU/mL, 0.9 % NaCl solution. Note: Due to the effective inactivation of ARB, the ARB survival curves at 265 nm demonstrated complete overlap in both the UV-LED alone and UV-LED/H_2O_2 systems. The ARB survival curves for the UV-LED alone, UV-LED/H_2O_2, and UV-LED/H_2O_2-TC systems at 280 nm exhibited complete overlap.

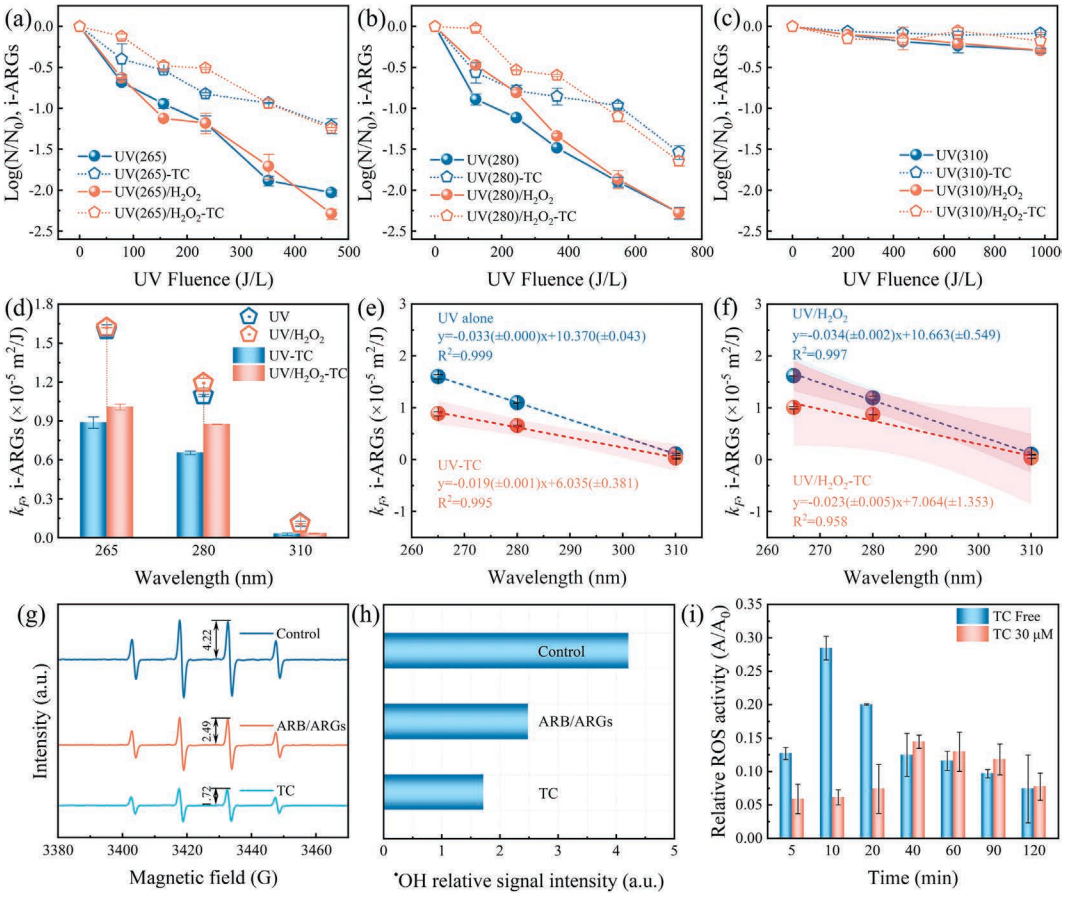


Fig. 3. The i-ARGs removal with or without TC coexistence in UV-LED alone and UV-LED/H_2O_2 systems at (a) 265 nm, (b) 280 nm and (c) 310 nm. (d) The k_F of i-ARGs with or without TC coexistence in UV-LED alone and UV-LED/H_2O_2 systems. Correlations between k_F of i-ARGs with UV-LED wavelengths in (e) UV-LED alone and (f) UV-LED/H_2O_2 systems with or without TC coexistence. The effect of ARB/ARGs and TC on (g) •OH EPR spectra and (h) their relative signal intensity in UV-LED/H_2O_2 system at 265 nm. (i) Relative intracellular ROS activity in UV-LED (265 nm)/H_2O_2 system with and without TC coexistence. Experiment conditions: TC 30 μmol/L, H_2O_2 10 mmol/L, ARB 3.5×10^6 CFU/mL, 0.9 % NaCl solution.

across the three wavelengths and decreased with increasing UV-LED wavelength. The •OH was proven to attack sugar backbone oxidized products, inducing DNA damage to facilitate ARGs removal [32]. However, •OH was difficult to penetrate the ARB membrane and it was easily consumed by cellular components, thus the UV-LED/H_2O_2 system with •OH as primary ROS was challenging to improve the i-ARGs removal efficiency (Fig. 3d) [33,34]. As expected, the coexistence of TC decreased the removal efficiency of i-ARGs, but the removal efficiency of i-ARGs maintained a high level at 265 nm.

In order to further elucidate the competitive mechanisms affecting the removal efficiencies of ARB/ARGs and TC in the UV-LED (265 nm)/H_2O_2 system, the generation of extracellular •OH and the activity of intracellular ROS within ARB were analyzed [35,36]. As depicted in Figs. 3g and h, the presence of ARB/ARGs or TC significantly decreased the EPR signal intensity of •OH in UV-LED/H_2O_2 system, indicating that both ARB/ARGs and TC actively scavenged •OH, and leading to pronounced competition for •OH. This competition for •OH impeded their respective inactivation and removal efficiencies. In addition, external stimuli such as UV photons and •OH

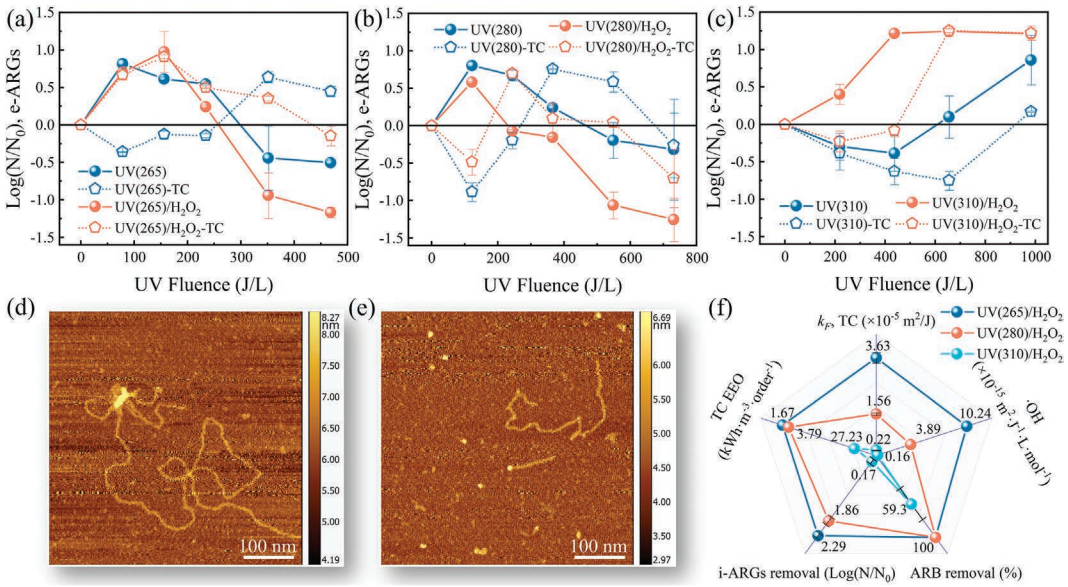


Fig. 4. The e-ARGs removal with or without TC coexistence in UV-LED alone and UV-LED/H_2O_2 system at (a) 265 nm, (b) 280 nm and (c) 310 nm. The AFM images of (d) initial i-ARGs and (e) treated with UV-LED (265 nm)/H_2O_2 system for 120 min. (f) The performance comparison for k_F and EEO of TC, ARB and ARGs removal efficiency, as well as ·OH yield in UV-LED/H_2O_2 system at three studied wavelengths. Experiment conditions: TC 30 μmol/L, H_2O_2 10 mmol/L, ARB 3.5×10^6 CFU/mL, 0.9 % NaCl solution.

directly triggered the oxidative stress response system in ARB, resulting in a rapid increase in intracellular ROS levels (Fig. 3i). This elevation disrupted the cellular redox balance, ultimately promoting ARB inactivation. However, the presence of TC reduced extracellular stimulation by consuming UV photons and ·OH, leading to a slow accumulation of intracellular ROS and a reduction in oxidative reactions within ARB cells. Therefore, TC decreased the inactivation efficiency of ARB by competing for UV photons and ·OH, while also reducing the intracellular ROS within ARB.

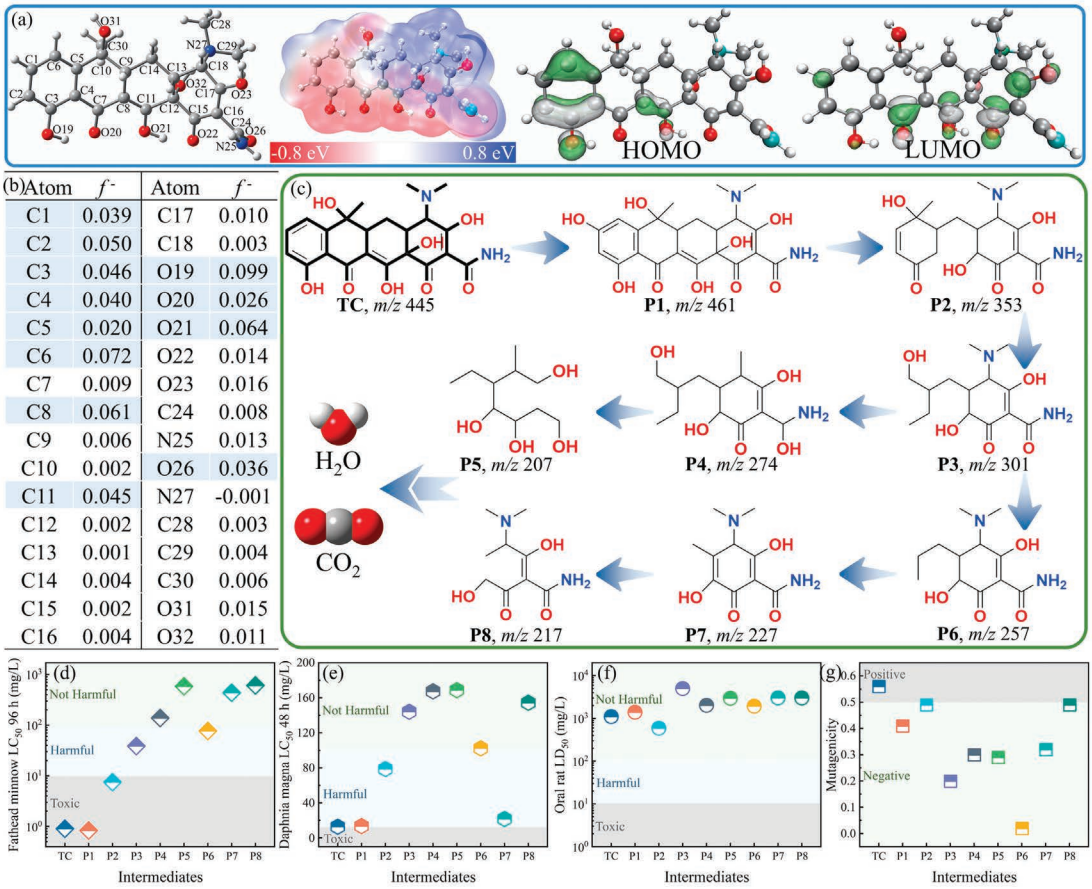
The efficiency of eliminating extracellular DNA (e-ARGs) was further assessed in both UV-LED alone and UV-LED/H_2O_2 systems. In systems with high ARGs removal potential (UV alone and UV/H_2O_2 system at 265 and 280 nm, UV/H_2O_2-TC system at 265 nm), e-ARGs initially increased due to the release of i-ARGs into extracellular environment because of the rapid inactivation of ARB (Figs. 4a and b). Subsequently, e-ARGs levels decreased as the UV dosage and ·OH yield increased with prolonged UV exposure. In systems with medium ARGs removal potential (UV-TC system at 265 and 280 nm, UV/H_2O_2-TC system at 280 nm), e-ARGs levels initially decreased due to the slow release of i-ARGs, then increased as gradually i-ARGs released. Eventually, e-ARGs levels decreased again with sustained UV irradiation, accumulation of ·OH and a reduction in rate of i-ARGs release (Figs. 4a and b). For systems with low ARGs removal potential, including UV alone, UV/H_2O_2, UV-TC and UV/H_2O_2-TC systems at 310 nm, two distinct trends were observed (Fig. 4c). In UV-LED alone system, the e-ARGs level initially decreased due to the delayed release of i-ARGs caused by ineffective ARB inactivation, but subsequently increased as the gradually released i-ARGs accumulated. In UV-LED/H_2O_2 system, the e-ARGs level consistently increased because of the continuous release of i-ARGs from ARB combined with the insufficient oxidative capacity for e-ARGs effective removal. In both UV-LED alone and UV-LED/H_2O_2 systems, the coexistence of TC intensified competition for photons and ·OH, delaying ARB inactivation and i-ARGs release, thus the e-ARGs level initially reduced and subsequently increased over time.

Furthermore, analysis of atomic force microscope (AFM) images of initial i-ARGs and those treated with UV-LED (265 nm)/H_2O_2 system for 120 min confirmed successful fragmentation of i-ARGs into small fragments, indicating their effective removal (Figs. 4d and e). Fig. 4f demonstrated the superior performance of UV-LED at 265 nm in terms of H_2O_2 activation for ·OH production, TC degradation, ARB and ARGs elimination, and overall energy efficiency. Consequently, UV-LED (265 nm)/H_2O_2 emerged as a promising technology for synchronous removal of antibiotics, ARB and ARGs with minimal energy consumption.

In UV-LED/H_2O_2 system, TC degradation was primarily driven by ·OH oxidation. The ·OH typically acted as an electrophilic, targeting e^--rich regions in organic pollutants [37–39]. In order to identify the vulnerable sites for ·OH attack and predict potential degradation intermediates of TC, the electrostatic potential, highest occupied molecular orbital (HOMO)-lowest unoccupied molecular orbital (LUMO) (Fig. 5a), and Fukui functions (f^-, Fig. 5b) were analyzed. The negative charge regions (red area) in the electrostatic potential of TC, concentrated at the C1-C8, O19-O21, O26 and O31 positions, align with HOMO orbitals and high f^- values. These regions represented potential sites vulnerable to electrophilic attacks, facilitating the capture of e^- by ·OH. Based on above analysis and mass spectrometry (MS) spectra (Fig. S8 in Supporting information), the possible degradation intermediates and pathway of TC in UV-LED/H_2O_2 systems were inferred.

The degradation process began with ·OH attacking the C1 position of TC, producing the hydroxylated intermediate P1 (Fig. 5c). Cleavage of the C3-C4 and C5-C6 bonds then detached resorcinol from **P1**, followed by C8=C11 bond cleavage, forming intermediate **P2**. The **P2** underwent further transformations, including ring-opening, demethylation, and decarbonylation, resulting in **P3**. The **P3** was further degraded through two distinct pathways: in the first pathway, removal of the tertiary amine (N27) from **P3** led to the formation of **P4**, followed by dehydroxylation, demethylation at C9, deamination at C24, and hydroxylation at C15 to yield the final product, **P5**. In the second pathway, demethylation and dehydroxylation at C8 and C9 in **P3** produced **P6**, which then underwent deethylation and C12-C13 bond cleavage to yield **P7**. Another final product, **P8**, was then formed through demethylation and C12-C13 bond cleavage of **P7**. Both final products, **P5** and **P8**, were eventually mineralized into CO_2 and H_2O.

Finally, the potential biological toxicity of TC and its degradation intermediates was predicted employing Toxicity Estimation Software Tool (T.E.S.T.) based on the quantitative structure-



Atom	f^-	Atom	f^-
C1	0.039	C17	0.010
C2	0.050	C18	0.003
C3	0.046	O19	0.099
C4	0.040	O20	0.026
C5	0.020	O21	0.064
C6	0.072	O22	0.014
C7	0.009	O23	0.016
C8	0.061	C24	0.008
C9	0.006	N25	0.013
C10	0.002	O26	0.036
C11	0.045	N27	-0.001
C12	0.002	C28	0.003
C13	0.001	C29	0.004
C14	0.004	C30	0.006
C15	0.002	O31	0.015
C16	0.004	O32	0.011

Fig. 5. (a) The structure, electrostatic potential distribution, HOMO and LUMO orbits of TC. (b) Fukui index (f^-) of TC. (c) Degradation pathway of TC in UV-LED/H_2O_2 system at 265 nm. The acutMe toxicity of (d) fathead minnow, (e) daphnia magna and (f) oral rat. (g) Mutagenicity of TC and its degradation intermediates. Experiment conditions: TC 30 μmol/L, H_2O_2 10 mmol/L, 0.9 % NaCl solution.

activity relationship (QSAR) method. The T.E.S.T. evaluated key toxicity indicators, including the *Fathead minnow* LC50 96 h, *Daphnia magna* LC50 48 h, *Oral rat* LD50 and mutagenicity. According to Figs. 5d-f, the toxicity of the degradation intermediates was generally lower than that of the parent compound, TC. For *Fathead minnow* and *Daphnia magna*, most intermediates fell into the categories of "Harmful" or "Not Harmful", and TC and its degradation intermediates were deemed "Not Harmful" for *Oral rat* exposure. This suggested that the UV-LED/H_2O_2 system significantly reduced toxicity for aquatic organisms. Additionally, the mutagenicity assessments were conducted to evaluate the potential hazards of TC and its intermediates (Fig. 5g). The TC was "mutagenicity positive", whereas all the degradation intermediates were found to be "mutagenicity negative". Thus, the UV-LED/H_2O_2 system was environmentally friendly, and it was an efficient and promising technology for antibiotic degradation, ARB inactivation and ARGs elimination.

This study investigated the wavelength dependence and competition interactions of TC and ARB/ARGs removal, as well as their simultaneous removal in UV-LED and UV-LED/H_2O_2 systems. The k_F of TC was determined by its ε_λ in UV-LED alone system and by $^{\bullet}OH$ yield UV-LED/H_2O_2 system within studied wavelengths (265, 280 and 310 nm). The k_F values for i-ARGs also exhibited a high correlation with UV-LED wavelengths in both systems ($R^2 = 0.997$–0.999), demonstrating a clear dependence on wavelength. The coexistence of TC alongside ARB/ARGs decreased the elimination efficiencies and increased the energy consumption each other. The competition between TC and ARB/ARGs for UV photons and $^{\bullet}OH$, along with the consequent reduction in intracellular ROS within ARB, resulted in a mutual inhibition of their removal efficiencies. The 265 nm proved as the optimal wavelength in UV-LED/H_2O_2 system for the simultaneous removal of TC, ARB, and ARGs, with minimal energy consumption. Additionally, the fragmentation of ARGs indicated the destruction of gene fragments, reducing the risk of gene transfer between organisms. The UV-LED/H_2O_2 system decreased the biotoxicity of TC wastewater, suggesting its potential for environmental safety. Overall, this research offered valuable insights into the competitive inhibition of antibiotics and ARB/ARGs in UV-LED/H_2O_2 system. The demonstrated degradation efficacy and energy efficiency position UV-LED/H_2O_2 system as a promising strategy for their simultaneous removal, contributing to enhanced antibiotic removal capability and addressing public health concerns associated with antibiotic resistance.

Declaration of competing interest

The authors declare that they have no known competing financial interests or personal relationships that could have appeared to influence the work reported in this paper.

CRediT authorship contribution statement

Jie Wang: Writing – original draft, Visualization, Methodology, Investigation, Data curation. **Jijie Zhang:** Validation, Investigation, Data curation. **Defang Ma:** Writing – review & editing, Resources, Project administration. **Zhenxiang Sun:** Investigation, Data curation. **Yan Wang:** Supervision, Resources. **Qinyan Yue:** Supervision, Resources, Project administration. **Yanwei Li:** Software. **Yue Gao:** Writing – review & editing, Supervision, Conceptualization. **Baoyu**

Gao: Writing – review & editing, Supervision, Resources, Conceptualization. **Xing Xu:** Writing – review & editing, Conceptualization.

Acknowledgments

The research was supported by Major Scientific and Technological Innovation Project of Shandong Province (No. 2020CXGC011204) and Qingdao Natural Science Foundation (No. 23–2–1–234-zyyd-jch). The authors would like to thank Chengcheng Ding (School of Environmental Science and Engineering, Shandong University) for the support of AFM test.

Supplementary materials

Supplementary material associated with this article can be found, in the online version, at doi:10.1016/j.cclet.2025.111209.

References

[1] Z. Zhang, Q. Zhang, T. Wang, et al., Nat. Commun. 13 (2022) 1553.
[2] S.K. Girijan, R. Paul, J.R. V, D. Pillai, Sci. Total Environ. 748 (2020) 141538.
[3] M. Li, K. Zhang, P. Wang, et al., App. Catal. B: Environ. 343 (2024) 123483.
[4] M. Qiao, G.G. Ying, A.C. Singer, Y.G. Zhu, Environ. Int. 110 (2018) 160–172.
[5] I.L. Brito, Nat. Rev. Microbiol. 19 (2021) 442–453.
[6] R. Singh, D.V. Naik, R.K. Dutta, P.K. Kanaujia, J. Clean. Prod. 266 (2020) 121986.
[7] Z.H. Li, L. Yuan, L. Wang, et al., J. Hazard. Mater. 423 (2022) 127088.
[8] Y. Xing, S. Wu, Y. Men, Environ. Sci. Technol. 54 (2020) 8770–8778.
[9] X. Lei, H. Zhao, C. Bai, et al., Chin. Chem. Lett. 36 (2025) 111550.
[10] J. Wang, J. Zhang, K. Guo, et al., Adv. Funct. Mater. 34 (2024) 2406790.
[11] J. Wang, H. Liu, D. Ma, et al., Chemosphere 268 (2021) 128796.
[12] J.A. Khan, A.D. Ogunniyi, G. Brunetti, et al., Process Saf. Environ. Prot. 202 (2025) 107589.
[13] K. Guo, Z. Wu, C. Chen, J. Fang, Acc. Chem. Res. 55 (2022) 286–297.
[14] J. Huang, Y. Wu, Y. Wu, et al., Sep. Purif. Technol. 284 (2022) 120264.
[15] H. Li, Z. Wang, J. Geng, Chin. Chem. Lett. 36 (2025) 110138.
[16] Z. Jing, Z. Lu, D. Santoro, et al., Chem. Eng. J. 447 (2022) 137584.
[17] J. Wang, H. Liu, Y. Gao, et al., Sci. Total Environ. 857 (2022) 159725.
[18] F.J. Barba, M. Koubaa, L. do Prado-Silva, et al., Trends Food Sci. Tech. 66 (2017) 20–35.
[19] D. Das, A. Bordoloi, M.P. Achary, et al., Sci. Total Environ. 833 (2022) 155205.
[20] T. Chen, C. Wang, S. Andrews, R. Hofmann, ACS ES&T Water 1 (2021) 1145–1152.
[21] H. Tang, Z. Liu, B. Hu, L. Zhu, Environ. Sci. Technol. 58 (2023) 1338–1348.
[22] G. Chu, W. Qi, W. Chen, et al., J. Hazard. Mater. 462 (2024) 132788.
[23] Y. Pei, A. Lei, S. Yang, et al., J. Hazard. Mater. 477 (2024) 135231.
[24] M.Y. Xu, C. Zeng, Y.L. Lin, et al., Water Res. 255 (2024) 121477.
[25] J. Wang, L. Pang, Y. Gao, et al., Sep. Purif. Technol. 327 (2023) 124974.
[26] J. Wang, H. Liu, Y. Wang, et al., Sep. Purif. Technol. 280 (2022) 119934.
[27] R. Yin, C. Shang, Water Res. 185 (2020) 116297.
[28] J. Wang, J. Zhang, K. Guo, et al., Water Res. 267 (2024) 122526.
[29] S. Giannakis, A. Gupta, C. Pulgarin, J. Imlay, Water Res. 221 (2022) 118740.
[30] S.E. Beck, H. Ryu, L.A. Boczek, et al., Water Res. 109 (2017) 207–216.
[31] J. Moreno-Andrés, M. Tierno-Galán, L. Romero-Martínez, et al., Water Res. 232 (2023) 119686.
[32] V.K. Sharma, X. Yu, T.J. McDonald, et al., Front. Environ. Sci. Eng. 13 (2019) 37.
[33] X. Meng, F. Li, L. Yi, et al., J. Hazard. Mater. 430 (2022) 128502.
[34] D. Das, A. Bordoloi, M.P. Achary, et al., Sci. Total Environ. 833 (2022) 155205.
[35] H. Hou, D. Zou, W. Shi, et al., Sci. Total Environ. 955 (2024) 176779.
[36] Y. Ahmed, J. Zhong, Z. Wang, et al., Environ. Sci. Technol. 56 (2022) 15156–15166.
[37] Y. Mu, Y. Chen, P. Chen, et al., ACS ES&T Water 1 (2021) 958–968.
[38] W. Liu, Y. Li, Y. Wang, et al., J. Hazard. Mater. 431 (2022) 128577.
[39] M. Dai, Q. Niu, S. Wu, et al., Environ. Chem. Lett. 22 (2024) 3059–3106.